

Finite Element Analysis of Normal Strength, High Strength and Hybrid Reinforced Concrete Beams

Nura Jasim Muhammed¹

Shaimaa T. Sakin²

Dunia sahib³

(Received 1 March 2012; accepted 6 May 2012)

Abstract

This paper presents the numerical study to simulate the flexural behavior of normal strength, high strength and hybrid reinforced concrete beams, under two points load with two different reinforcement ratio. The hybrid beam consists of two layers: the compressive layer is made of high strength concrete, and the tension layer is made of normal strength concrete. The simulation was done with a finite element model using the commercial finite element code, ANSYS (v.9.0). The concrete component material is modeled, the internal steel reinforcement modeled using "LINK" elements. The modeled behavior shown a good agreement with the experimental data. The maximum percentage difference in ultimate load-carrying capacity is 8% at the ultimate load level. Analytical study also included the effect of increasing the depth of the normal strength concrete for the hybrid reinforced concrete beam and the effect of increasing the compressive strength for high strength concrete and normal strength concrete respectively on the behavior and the load carrying capacity of the hybrid reinforced concrete beams.

Key Words: Reinforced concrete beam, finite element modeling, and Hybrid reinforced concrete beam.

التحليل بطريقة العناصر المحددة للعتبات الخرسانية المسلحة الاعتيادية المقاومة والعالية المقاومة والمهجينة

دنيه صاحب

شيماء طارق ساكن

نورا جاسم محمد

الخلاصة

ان هذا البحث يقدم دراسة عددية لتمثيل سلوك الانثناء لنماذج من العتبات الخرسانية المسلحة المصنوعة من الخرسانة الاعتيادية والعالية المقاومة و المهجنة تحت تأثير الحمل في تقطين ونسبتين مختلفتين من التسليح. الاعتاب المهجنة تتكون من طبقتين: الاولى مكونة من الخرسانة الاعتيادية في منطقة الشد والثانية من الخرسانة عالية المقاومة في منطقة الانضغاط. لقد تم تطوير نموذج التحليل العددي باستخدام برنامج ANSYS (الاصدار 9). لقد تم تمثيل الخرسانة باستخدام عناصر ثلاثية الابعاد تأخذ بنظر الاعتبار تأثير التصدعات و باقي الخواص اللاخطية. كما تم استعمال عناصر ربط لتمثيل حديد التسليح وقد اظهرت النتائج المستخرجة من التحليل العددي تقارب جيد مع النتائج العملية. بحيث أكثر فرق في التحمل الأقصى جاء 8%.

كما تضمنت الدراسة النظرية تأثير زيادة عمق الخرسانة الاعتيادية في الاعتاب المهجنة وتأثير زيادة مقاومة انضغاط الخرسانة عالية المقاومة و الخرسانة الاعتيادية على سلوك وقمة الحمل الأقصى للاعتاب الخرسانية المهجنة.

1- INTRODUCTION:

Advances in concrete technology have now made practical the use of concrete for strength up to (90 – 100 N/mm²). This concrete, with very high compressive strength is characterized by its high cost compared to normal strength concrete. Thus, the use of such type of concrete must be justified from the economical point of view⁽¹⁾.

Hybrid layered systems of various strength materials in this study, as the hybrid beams consist of two layers: the compressive layer which is made by HSC, and the tension layer which is made of

¹Asst. Lec.Civil Engineering Dept. College of Engineering, Al -Mustancirya University.

²Asst. Lec.Civil Engineering Dept. College of Engineering, Al -Mustancirya University

³ Asst. Lec.Department of Highway Engineering College of Engineering, Al -Mustancirya University.

NSC. The final (hybrid) cross-section combines both traditional (concrete) and new high strength to create a highly optimized structure⁽²⁾.

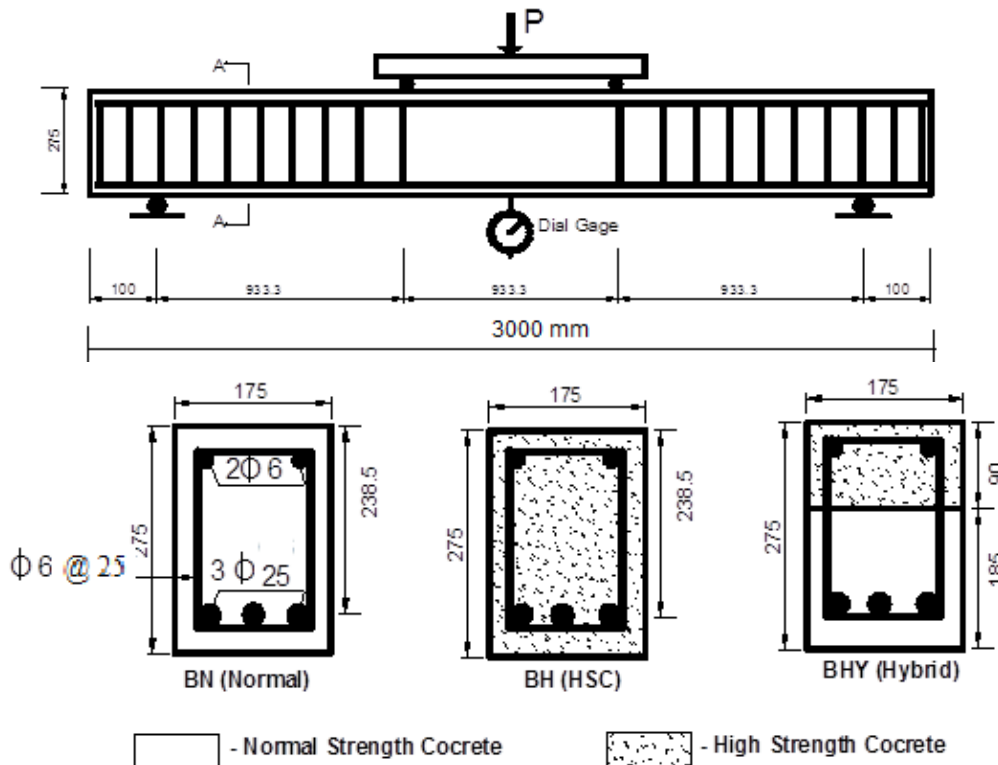
This paper presents three dimensional material nonlinear finite element (FE) model, developed with commercial finite element package, ANSYS 9, to simulate the behavior of reinforced concrete beam specimens of normal strength, high strength and hybrid reinforced concrete beams tested by two concentrated point load. The obtained results from the FE analysis are compared with experimental data for the RC beams (Kareem Sh. 2006⁽²⁾). The results are presented in terms of ultimate load carrying capacity and deformation characteristics. Finally, the accuracy and validity of the model were investigated.

2- GEOMETRY:

Six specimens of Kareem Sh. beams 2006⁽²⁾ are chosen for the finite element analysis as shown in Figure (1). The beams are made of normal strength concrete (BN) (22.5 N/mm²), while beams made of high strength concrete (BH) (72.5 N/mm²), and the beams made of two different concrete mixes (BHY) (22.3 and 73.7 N/mm²), the (22.3 N/mm²) mix is for casting the lower (185 mm) of the beams and the other is high strength concrete (73.7 N/mm²) for the upper (90 mm) of the beams.

The beams are designed to fail in flexure, two different reinforcement ratios (1.43% and 3.56%) and reinforcement in the form of vertical stirrups is used to prevent shear failure.

The dimensions of all the beams are geometrically similar, having rectangular cross-section, of dimension (175×275 ×3000) mm. As shown in Figure (1). The beams tested are simply supported over (2800) mm span and loaded at two points having a distance of (933.3) mm between them.



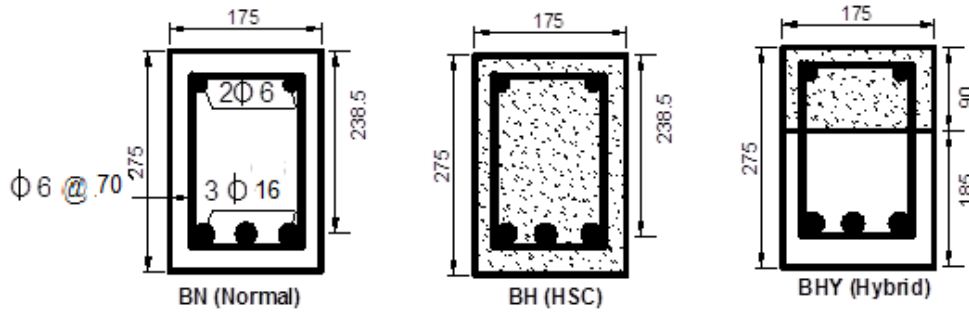


Figure (1): Loading and Specimen Details (All dimensions are in (mm))

3- FINITE ELEMENT MODEL:

3- 1- Element types:

3-1-1 Concrete:

An eight-node solid element, Solid65, was used to model the concrete. Each node has three degrees of freedom in x, y, and z directions. Plastic deformation, cracking in three orthogonal directions, and crushing of the elements are allowable. Figure (2) show the geometry and node locations for this element.

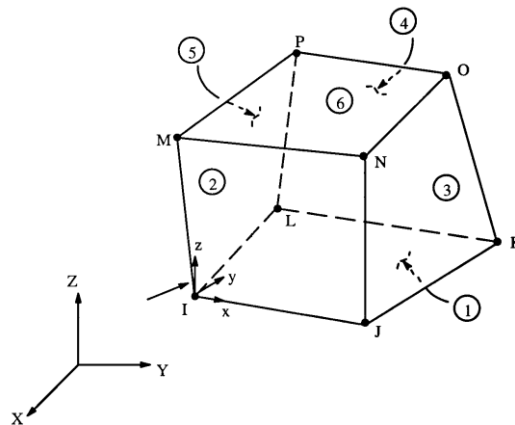


Figure (2): Solid65 – 3-D solid ⁽³⁾.

For reinforced concrete, ANSYS requires input data for material properties as follows:

- Elastic modulus (E_c).
- Ultimate uniaxial compressive strength (f'_c).
- Ultimate uniaxial tensile strength (modulus of rupture, f_r).
- Poisson’s ratio (ν).
- Shear transfer coefficient (β_o, β_c).

the modulus of elasticity, E_c , can be calculated with a reasonable accuracy from the empirical formula (ACI code 318-2005) ⁽⁴⁾.

$$E_c = 4700 \sqrt{f'_c} \dots\dots\dots (1) \quad (f'_c \text{ in MPa})$$

The modulus of rupture f_r is taken as $(0.7\sqrt{f'_c})$. A shear transfer coefficient (β) is introduced in order to estimate the ability of concrete to transfer shear force across the crack interface. This coefficient represents a shear strength reduction factor for concrete across the crack face ⁽³⁾. The shear transfer coefficient used in this study were 0.2 and 0.3 for the case of open crack (β_o) and closed crack (β_c) respectively.

The uniaxial stress-strain relationship for concrete in compression is required by the program. The numerical expressions equations (2, 3, and 4) were used along to construct the uniaxial compressive stress-strain curve of concrete in this study (Desayi and Krishnan 1964)⁽⁵⁾, and stress-strain curve for normal weight concrete are shown in figure (3).

$$f_c = \frac{\varepsilon E_c}{1 + \left(\frac{\varepsilon}{\varepsilon_o}\right)^2} \quad \text{for} \quad \varepsilon_1 \leq \varepsilon \leq \varepsilon_o \dots \dots \dots (2)$$

$$\varepsilon_o = \frac{2f'_c}{E_c} \dots \dots \dots (3)$$

$$E_c = \frac{\sigma}{\varepsilon} \quad \text{for} \quad 0 \leq \varepsilon \leq \varepsilon_1 \dots \dots \dots (4)$$

Where:

σ = stress at any strain ε , N/mm².

ε = strain at stress f .

ε_o = strain at the ultimate compressive strength f'_c .

ε_1 = strain corresponding to stress $0.3f'_c$.

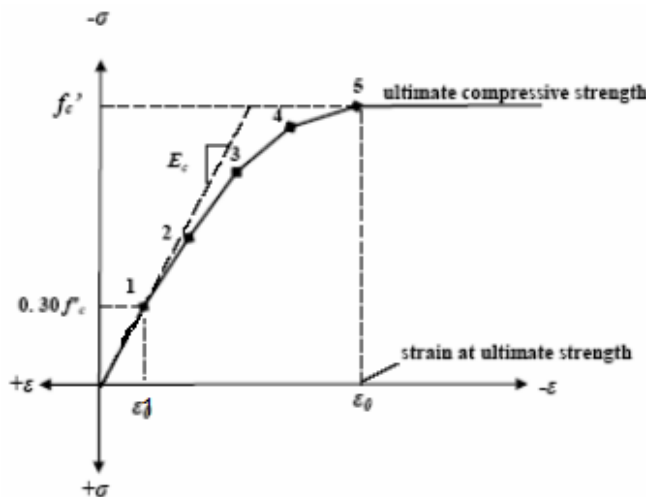


Figure (3): Simplified Compressive Uniaxial Stress- Strain Curve for Concrete [6]

For the convergence nonlinear solution algorithm, the multi-linear curves were used. The summary of Material properties for all concrete types is shown in Table (1).

Table (1): The summary of Material properties for all concrete types

| Material Properties | Concrete Types | | | |
|------------------------------------|----------------|-----------|-------------------|-------|
| | BN NSC | BH HSC | HYB NSC HSC | |
| Compressive strength f'_c (MPa) | 22.5 | 72.5 | 22.3 | 73.7 |
| Young's modulus E_c (MPa) | 23640 | 38820 | 24220 | 42530 |
| Tensile strength f_r (MPa) | 3.6 | 21.75 | 3.64 | 6 |
| Poisson's ratio ν^* | 0.2 | 0.2 | 0.2 | 0.2 |

* Assumed

3-1.2 Steel reinforcement:

To model the steel reinforcement we used Link8 element. This element has two nodes with three degrees of freedom in nodal x, y and z directions and capable of plastic deformation. A perfect bond between the concrete and steel reinforcement is considered. Figure 4 shows the geometry and load locations of the element.

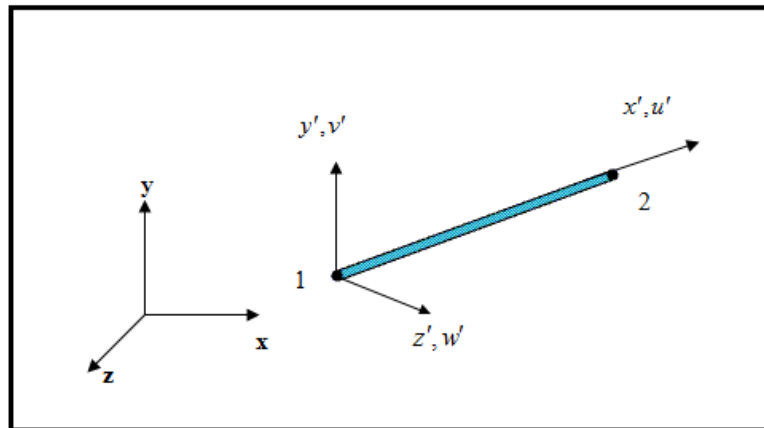


Figure (4): Link8 – 3-D spar ⁽³⁾

The steel reinforcement was connected between nodes of each adjacent concrete solid element, so the two materials shared the same nodes. The steel reinforcement for the FE model is assumed to be elastic- perfectly plastic and identical in tension and compression as shown in Figure (5). Tables 2 reports material properties for the steel reinforcement for all beams models.

Table (2): Material properties of the steel reinforcement

| Nominal diameter (mm) | Poisson's ratio ν^* | Modulus of elasticity (GPa)* | f_y (MPa) | f_u (MPa) |
|-----------------------|-------------------------|------------------------------|-------------|-------------|
| 6 | 0.3 | 200 | 382.5 | 545.4 |
| 16 | 0.3 | 200 | 420 | 635.3 |
| 25 | 0.3 | 200 | 444.9 | 708.6 |

*Assumed

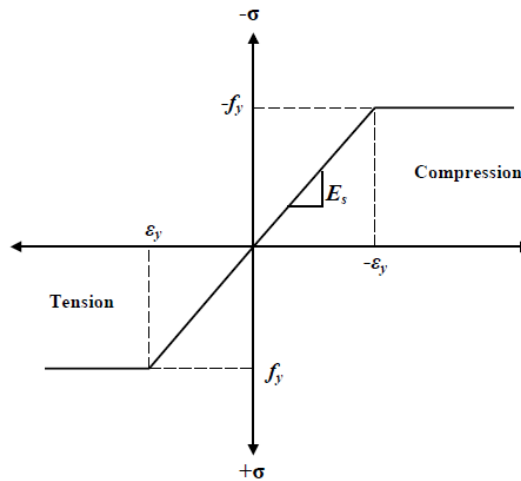


Figure (5): Stress-strain curve for steel reinforcement

4- FINITE ELEMENT IDEALIZATION:

By taking advantage of the symmetry of the three beam’s geometry and loading, a half of the entire model beam was used for the finite element analysis.

In order to represent the concrete material, the reinforced concrete beams are modeled by (5760) 8-node brick elements. While (2263) three-dimensional two-node bar elements (link8) were used to model the reinforcement bars which share with concrete elements in the same nodes.

Perfect bond was assumed between normal and high strength concrete for hybrid reinforced concrete beams.

The final step is applying the boundary conditions and the loads. There are two boundary conditions one for supports and the other for symmetry. For the support, the point of supports is constrained in the x and y-directions (hinge support). For the symmetry, one plane of symmetry exist, and at a plane of symmetry the displacement in the direction perpendicular to that plane was held at zero value ($U_z=0$). The external load is represented by equivalent nodal loads.

The boundary conditions and loading of hybrid reinforced concrete beam of the finite element mesh, are shown in Figure (6) and Figure (7).

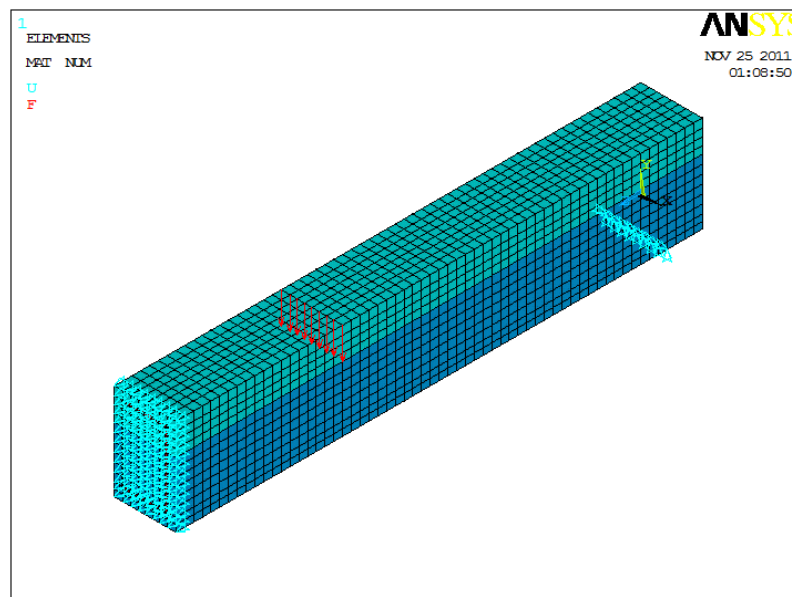
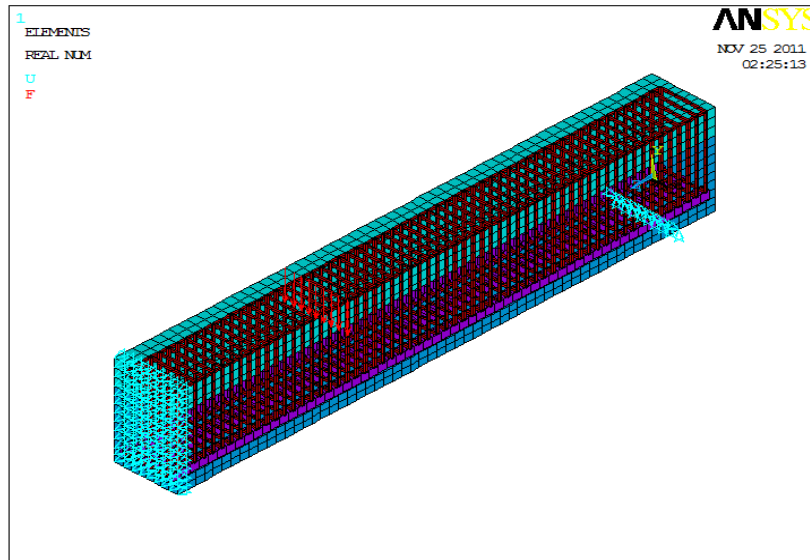
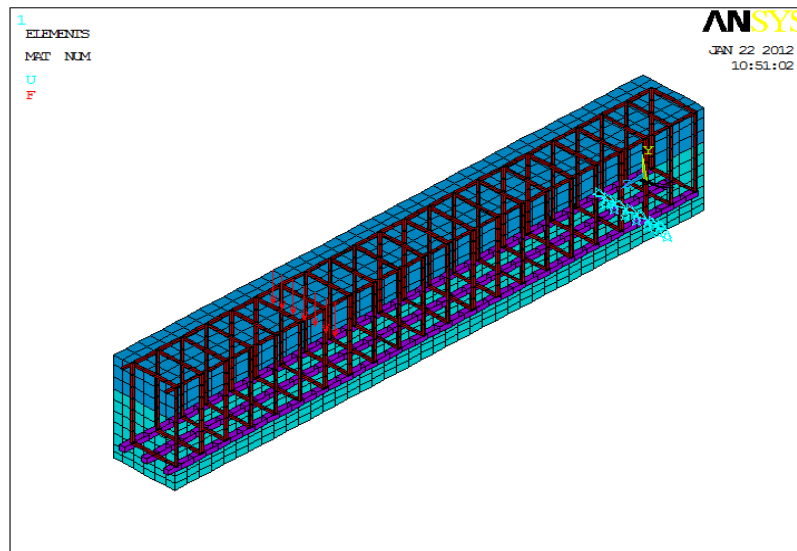


Figure (6): FE mesh, boundary condition and loading for hybrid reinforced concrete beam



a. (3φ25mm)



b. (3φ16 mm)

Figure (7): modeling of steel reinforced of hybrid reinforced concrete beams

To carry out the nonlinear analysis, the calculation was conducted by using 8-point ($2 \times 2 \times 2$) integration rule, and full Newton-Raphson method, and a convergence tolerance of (1%) is used. For applying the external load we used the uniform increments load. The last applied load steps represents the final loads for the finite element models before the solution diverges due to numerous cracks and large deflections.

5- RESULTS AND DISCUSSION:

The validation of the FE models was conducted by comparing the modeled load carrying capacity and load-deflection with the experimental results for normal, high and hybrid reinforced concrete

beams specimens. The finite element load-deflection response, obtained for the beams, BN, BH and BHY for two reinforcement ratios (1.43% and 3.95%) are shown in Figures (8), (9) and (10) respectively along with the corresponding experimental results. The behavior of the numerical models agrees well with the reported experimental observations throughout the whole loading process as can be seen from the load – deflection curves, some differences between the experimental and finite element beams appeared in curves and this may be caused by several factors that lead to higher stiffness in the finite element models. The finite element analyses assumes the bond between the concrete and steel reinforcing is perfect, but in the reality the assumption would not be true because slip may occurs, therefore the composite action between the concrete and steel reinforcing is lost in the actual beams. Also the microcracks formed by drying shrinkage and handling are also may be present in the concrete to some degree. The aforementioned reasons would reduce the stiffness of the actual beams, while the finite element models do not take in consideration the microcracks which is not incorporated in the models. Also, the perfect bond between the two concrete types for hybrid beams which appeared especially after yield point may lead to different results. The experimental and the analytical load-carrying capacity for the beams and the ratio between them are shown in Table (3).

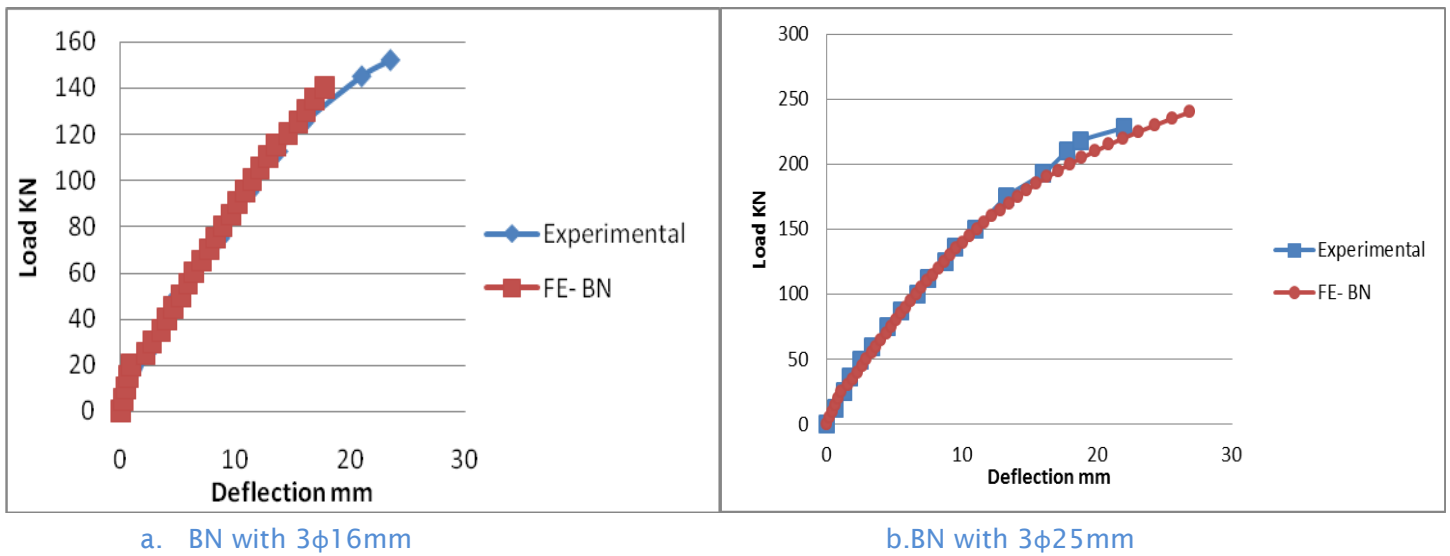
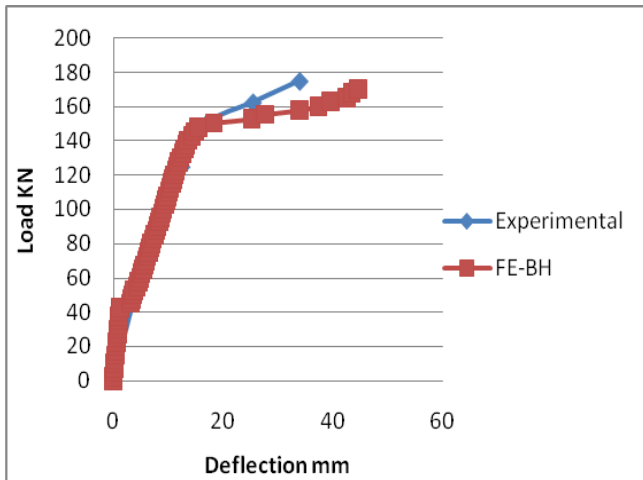
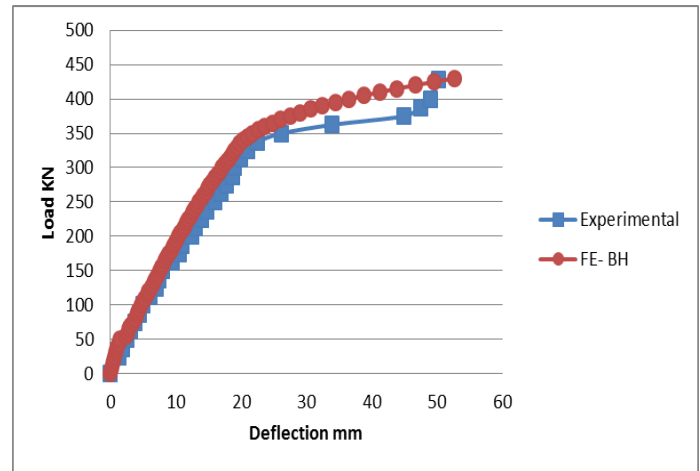


Figure (8):Load-deflection behavior of BN beams

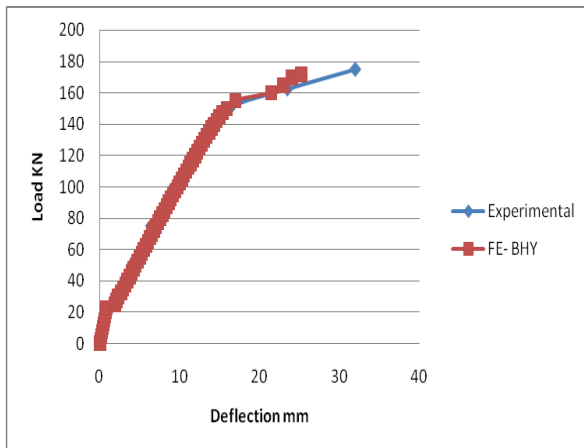


a. BH with 3φ16mm

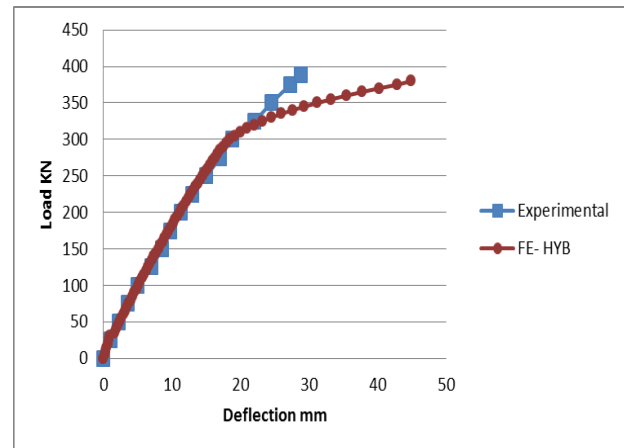


b. BH with 3φ25mm

Figure (9): Load-deflection behavior of BH beams



a. BHY with 3φ16mm



b. BHY with 3φ25mm

Figure (10): Load-deflection behavior of BHY beams

Table (3): Experimental and predicted failure loads for beams BN, BH and BHY

| Beam | Ultimate load (kN) | | FE/Exp. | Max. Deflection | | FE/Exp. |
|--------|--------------------|-----|---------|-----------------|-------|---------|
| | Exp. | FE | | Exp. | FE | |
| BNφ25 | 228 | 240 | 1.05 | 22 | 26.88 | 1.22 |
| BHφ25 | 428 | 435 | 1.01 | 50.3 | 56.1 | 1.11 |
| BHYφ25 | 388 | 380 | 0.98 | 28.75 | 44.9 | 1.56 |
| BNφ16 | 152 | 140 | 0.92 | 23.5 | 17.8 | 0.75 |
| BHφ16 | 175 | 170 | 0.97 | 34 | 44.7 | 1.31 |
| BHYφ16 | 175 | 172 | 0.98 | 32 | 25.3 | 0.79 |

6- Effect of some parameters on behavior of hybrid beams

The behavior of a hybrid beams are affected by many parameters. In the current study the beams (BHY) have been employed in a numerical study to demonstrate the effects of some parameters on the nonlinear finite element solution. These parameters include the following:

- The effect of changing depth of normal strength concrete.
- The Effect of Increasing Compressive Strength of Concrete.

The effects of each of the above-mentioned parameters are discussed below.

6-1 The Effect Of Changing The Depth Of Normal Strength Concrete:

In order to investigate the effect of changing the depth of normal strength concrete (h) on the behavior of hybrid reinforced concrete beams, the hybrid beams BHY have been analyzed with different values of (h). Figure (11) and Figure (12) show the study of this effect on the Load-Deflection behavior.

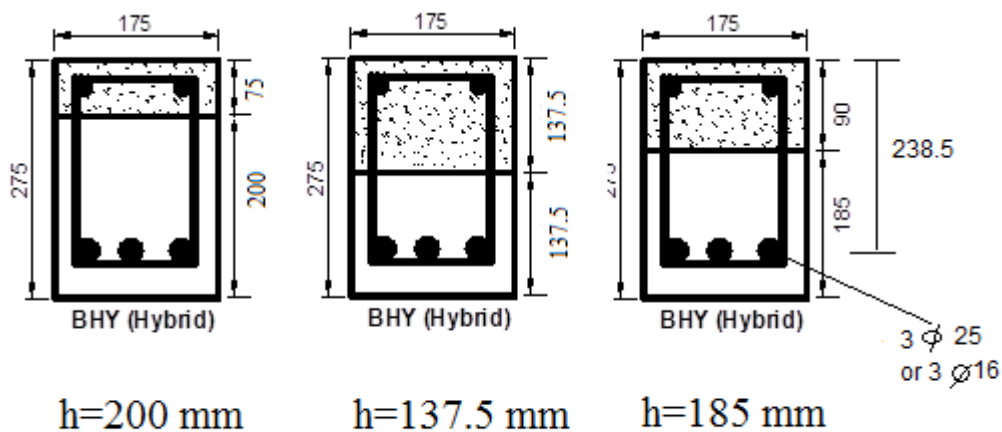
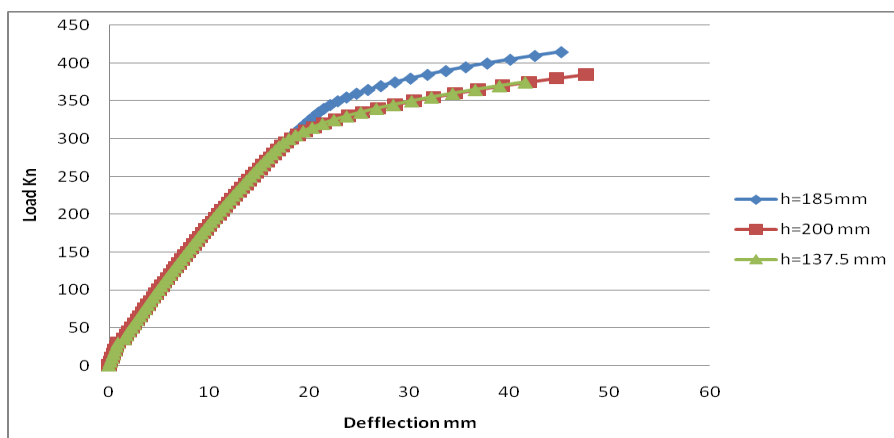
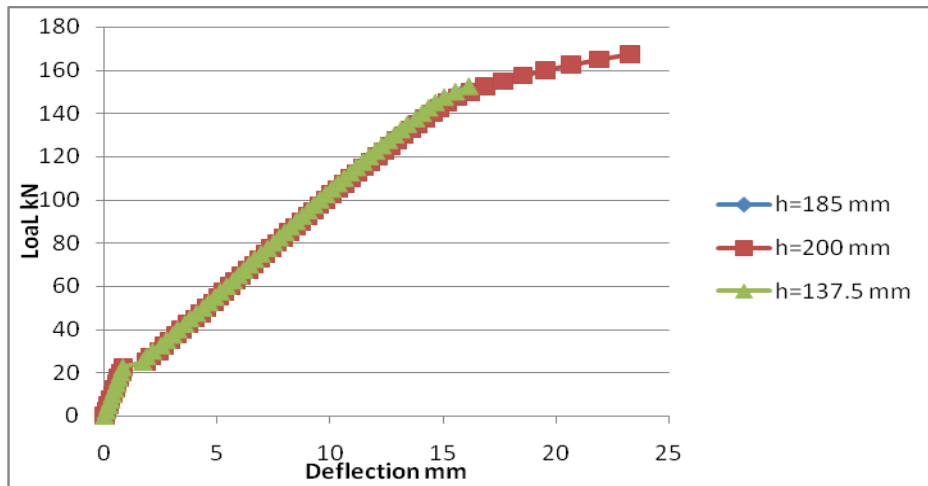


Figure (11):The change in depth of NSC



A.BHY with 3φ25mm



B.BHY with $3\phi 16\text{mm}$

Figure (12): The effect of changing depth of normal strength concrete on the BHY beams

According to the results of the analysis, the following observation may be noted for BHY with $3\phi 25$ (3.56% steel ratio):

- ◆ Increasing the depth of normal strength concrete for the hybrid reinforced concrete beam from (h=185mm) to (h= 200 mm), decreased the ultimate load by (7.2%).
- ◆ Decreasing the depth of normal strength concrete for the hybrid reinforced concrete beam from (h=185mm) to (h= 137.5 mm) , decreased the ultimate load by (9.6%).

According to the results of the analysis, the following observation may be noted for HBY with $3\phi 16$ (1.43% steel ratio):

- ◆ Increasing the depth of normal strength concrete for the hybrid reinforced concrete beam from (h=185mm) to (h= 200 mm), increased the ultimate load by (11.3%).
- ◆ Decreasing the depth of normal strength concrete for the hybrid reinforced concrete beam from (h=185mm) to (h= 137.5 mm), increased the ultimate load by (1.67%).

6-2 The Effect of Increasing the Compressive Strength of Concrete:

Figure (13), (14),(15) and(16) shows the effect of increasing the compressive strength of normal and high strength concrete for HYB beams with ($\rho=3.56\%$ and 1.43%) respectively on the behavior of the hybrid reinforced concrete beam BHY. Based on the results of the analysis for HBY with $\rho=3.56$, the following observation may be recorded:

- With respect to the beam BHY with originally $f'c = 22.3\text{MPa}$ for the normal strength concrete, the effect of increasing $f'c$ to 30MPa , caused an increase in the ultimate load by about (3.9%).
- Similarly, the effect of increasing the compressive strength of normal strength concrete to $f'c = 40\text{MPa}$, caused an increase in the ultimate load by about (5.2%).

- Increasing the compressive strength of the high strength concrete to $f'c=95$ MPa with respect to the original compressive strength $f'c =73.7$ MPa, cause an increase in the ultimate load by (3.9%).
- Similarly, the effect of increasing the compressive strength of high strength concrete to $f'c =120$ MPa, caused an increase in the ultimate load by about (5.2%).

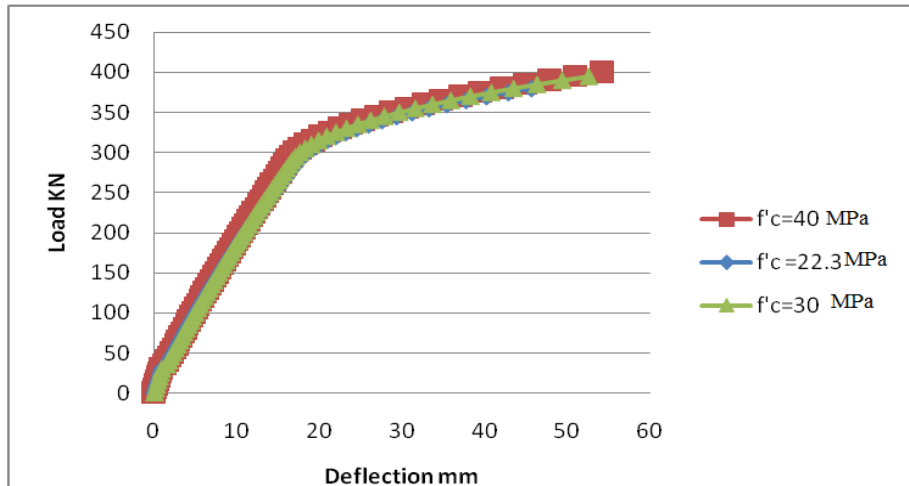


Figure (13) : Effect of increasing the compressive strength of normal strength concrete for the BHY beam with $\rho=3.56$ %.

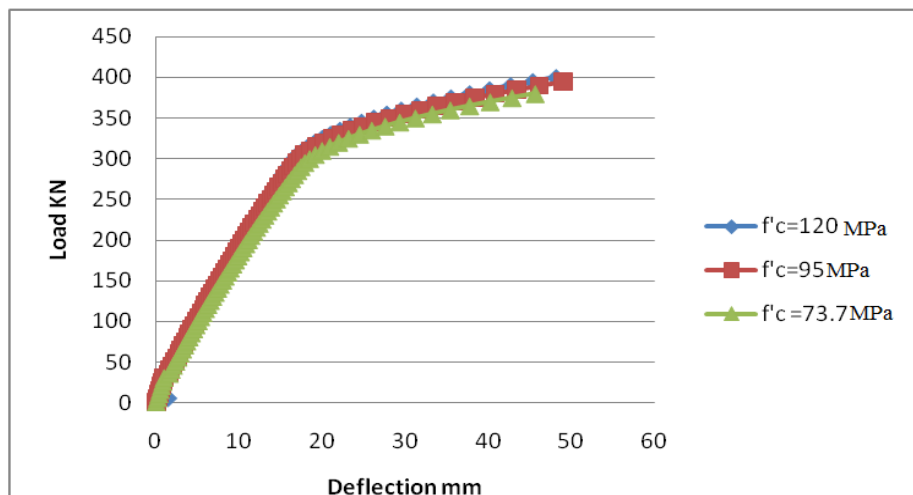


Figure (14): Effect of increasing the compressive strength of high strength concrete for the BHY beam with $\rho=3.56$ %.

Based on the results of the analysis for HBY with $\rho= 1.43$, the following observation may be recorded:

- With respect to the beam BHY with originally $f'c =22$ MPa for the normal strength concrete, the effect of increasing $f'c$ to 30MPa, caused an increase in the ultimate load by about (1.67%).
- Similarly, the effect of increasing the compressive strength of normal strength concrete $f'c =40$ MPa, caused an increase in the ultimate load by about (18.33%).

- Increasing the compressive strength of the high strength concrete to $f'c=95$ MPa with respect to the original compressive strength $f'c =71.1$ MPa, cause an increase in the ultimate load by (5%).
- Similarly, the effect of increasing the compressive strength of high strength concrete to $f'c=120$ MPa, caused an increase in the ultimate load by about (6.67%)

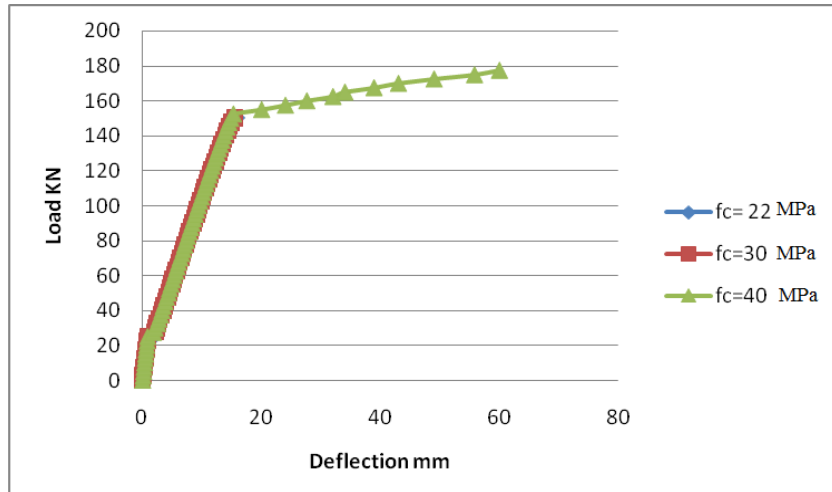


Figure (5): Effect of increasing the compressive strength of normal strength concrete for the BHY beam with $\rho=1.43$ %.

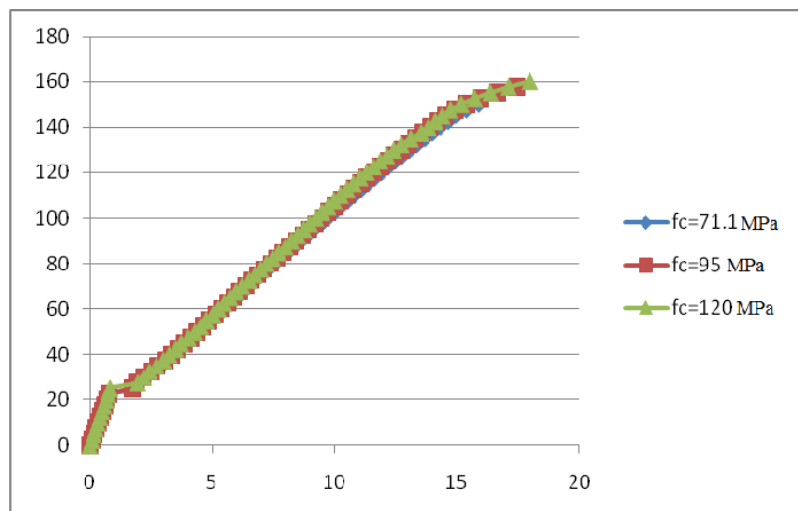


Figure (16): Effect of increasing the compressive strength of high strength concrete for the BHY beam with $\rho=1.43$ %.

Conclusion:

1. According to the results of the available experimental tests with comparison with the results obtained from the finite element analysis by (ANSYS) it is shown that the computer modeling can be used efficiently to predict the structural response and the load carrying capacity of such beams.
2. Increasing the depth of normal strength concrete for the hybrid concrete beam (with $\rho=3.56$ %) by 8% cause a decrease of the ultimate load by (7.2%), while decreasing the depth of normal strength concrete by 25.6% cause a 9.6% decrease in the ultimate load caring capacity.

3. Increasing the depth of normal strength concrete for the hybrid concrete beam (with $\rho=1.43\%$) by 8% cause a increase of the ultimate load by (11.3%), and decreasing the depth of normal strength concrete by 25.6% cause a 1.67% increase in the ultimate load caring capacity.

4. The finite element solution reveals that increasing the compressive strength of concrete causes an increase in the ultimate load carrying capacity. For the studied cases it is found that increasing $f'c$ of the normal strength concrete for the hybrid beams in the range of (34%-79%) causes an increasing in the load capacity by (3.9%-5.2%) and (1.67% -18.33%) for ($\rho=3.56\%$ and 1.43%) respectively .

5. Increasing ($f'c$) of the high strength concrete for the hybrid beams in the range of (29%-63%) causes an increase in the ultimate load capacity by (3.9%-5.2%) and (5%-6.67%) for ($\rho=3.56\%$ and 1.43%) respectively.

References:

- 1) Abrishami, H.H, Cook, W.D., and Mithchel, D., "*Influence of Epoxy-Coated Reinforcement on Response of NSC and HSC Beams*", ACI Structural Journal, Vol.92, No.2, March-April 1955, pp.157-166.
- 2) Kareem Sh. S. "*Flexural Behavior of Hybrid Reinforced Concrete Beams*", M.Sc. thesis, Al- Mustansirya University, Iraq, 2006.
- 3) "*ANSYS Manual*", Version 9.0, U.S.A. 2004
- 4) ACI Committee 318, "*Building Code Requirements for Structural concrete (ACI 318-2005, ACI 318R-2005)*", American Concrete Institute, 2005.
- 5) *Desayi, P. and Krishnan, S., "Equation for the Stress-Strain Curve of Concrete,"* Journal of the American Concrete Institute, 61, pp. 345-350, March 1964.
- 6) Bangash, M. Y. H., "*Concrete and Concrete Structures: Numerical Modeling and Applications*", Elsevier Science Publishers Ltd., London, England, 1989.